Quarterly Progress Report
July-September, 2002

Development of a New Approach for the Evaluation of Mechanical Reliability of Ceramic Gas Turbine Components

J. P. Singh, K. Sharma, and P. S. Shankar
Argonne National Laboratory, Argonne, IL 60439
Phone: (630) 252-5123, E-mail: jpsingh@anl.gov

M. K. Ferber and M. Lance
Oak Ridge National Laboratory, Oak Ridge TN 37831

Objective: The purpose of this proposed research is to develop novel test methodology for the performance characterization of advanced structural ceramics for gas turbine applications. Specifically, effort will concentrate on evaluating mechanical properties, identifying critical flaws, and characterizing failure modes/mechanisms to develop and verify the test methodology.

Background: High performance Si_3N_4 ceramics with reinforcing agents and refined microstructures are leading candidates for high temperature structural applications in advanced gas turbines components. Although Si_3N_4 materials have been used in high temperature structural applications, the ceramic components exposed in engine tests have not exhibited the required reliability. This lack of reliability is believed to be due to the data obtained from laboratory test specimens that are used for life prediction of the actual turbine components. The problem, apparently, is due to the fact that these test specimens are usually fabricated differently from the turbine components. Furthermore, the test specimens are generally machined and ground to obtain the required dimensions for a standard test. Thus, the test specimens may have different surface characteristics, including strength controlling critical flaws, than those of the actual components with as-processed surfaces. This may lead to property variation between the test specimens and the components. An approach to avoiding this problem is to evaluate the material properties by using miniature biaxial test specimens directly machined from actual components.

To this end, research has focused in two primary areas: (A) mechanical property evaluation using miniature disk specimens and (B) verifying the analytical stress solutions by stress measurement using piezofluorescence. Specifically, effort has concentrated on (1) evaluating the effects of surface machining on the nature of critical flaws and resulting strength of Si_3N_4 specimens, (2) identifying and characterizing critical flaws, (3) establishing correlation between strength characteristics of the specimens with as-processed and machined surfaces, and (4) evaluating the applicability of miniature biaxial disk specimens for predicting mechanical performance of turbine components. Progress to date is summarized below.

Technical Highlights:

(A) Mechanical properties evaluation using miniature disk specimens (J. P. Singh, K. Sharma, and P. S. Shankar, Argonne National Laboratory)

In the previous quarterly report (April-June 2002), results of four-point flexure testing and fractographic evaluations of the AS800 Si_3N_4 (Honeywell Inc.) specimens were reported. It was observed that the as-processed specimens exhibited lower flexure strength (459±102 MPa) as compared to the ground specimens (689±67 MPa). This was shown to be due to the different critical flaw characteristics: agglomerate defects in as-processed specimens as compared to the machining flaws in ground specimens.

The present report discusses the results of biaxial flexure testing of AS800 Si_3N_4 specimens in continuation of meeting the program objectives. Miniature biaxial disk specimens (6.5 mm diameter and 0.5 mm thickness) were machined from the broken halves of the four-point flexure bars by first grinding and then core drilling the flexure bars to obtain the desired thickness and diameter. Five sets of biaxial specimens were tested, one in the as-processed condition and four in the ground condition. Of the four sets of ground specimens, three were prepared by grinding one face of the bars with diamond powders of different sizes (100 μm, 23 μm and 9 μm) and the fourth set was ground with 25 μm alumina powder. The as-processed and ground faces of the specimens were used as tensile surfaces during the biaxial experiments.

Fig. 1 shows the pictorial view of the ball-on-ring fixture used for the biaxial experiments. The specimen is supported by three balls of 1 mm diameter, positioned 120° apart on a 5 mm diameter circle. The load is applied to the specimen from the top by another 1 mm diameter ball that is attached to the cross-head of an Instron mechanical test system. The biaxial flexure strength of the disk specimens was calculated by using equation (1) [1]:

$$\sigma_{max} = \{3P(1+\upsilon)/4\eth t^2\}\ \{1+2\ \ln(a/b)+((1-\upsilon)/\ (1+\upsilon))\ (1-b^2/2a^2)\ (a^2/R^2)\} \qquad (1)$$

where, P is the maximum sustained load, R is the specimen radius, t is the specimen thickness, υ is the Poisson ratio, a is the radius of the support ball ring (=2.5 mm) and b is the effective radius of contact (≈t/3) of the loading ball on the specimen.

Fig. 2 shows the measured biaxial flexure strength as a function of surface finish for the five sets of miniature biaxial specimens tested. The solid horizontal line in Fig. 2 corresponds to the strength of the as-processed specimen (858±68 MPa). Fig. 2 shows that the biaxial strength of the ground specimens increases as the surface finish becomes finer, i.e., from 717±43 MPa with 100 μm diamond finish to 875±89 MPa with 23 μm diamond finish. This suggests that the critical flaw size is larger in the specimens ground with 100 μm diamond powder as compared to those ground with 23 μm diamond powder. Furthermore, the biaxial strength of the specimens ground with 9 μm diamond powder is 869±52 MPa indicating that the strength appears to become independent of

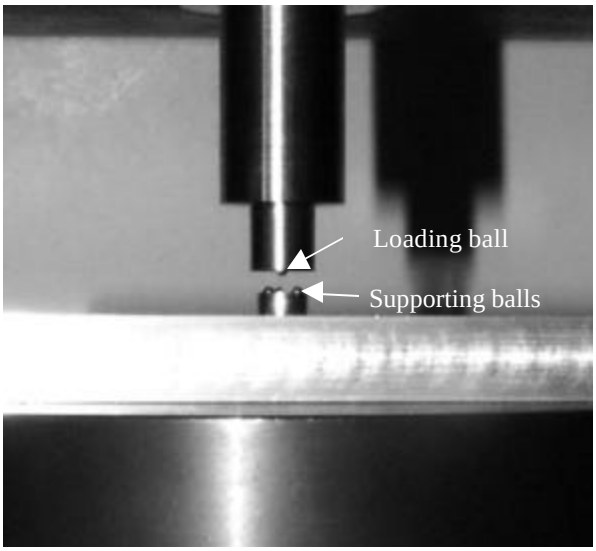

Figure 1. Fixture used for ball-on-ring biaxial flexure testing.

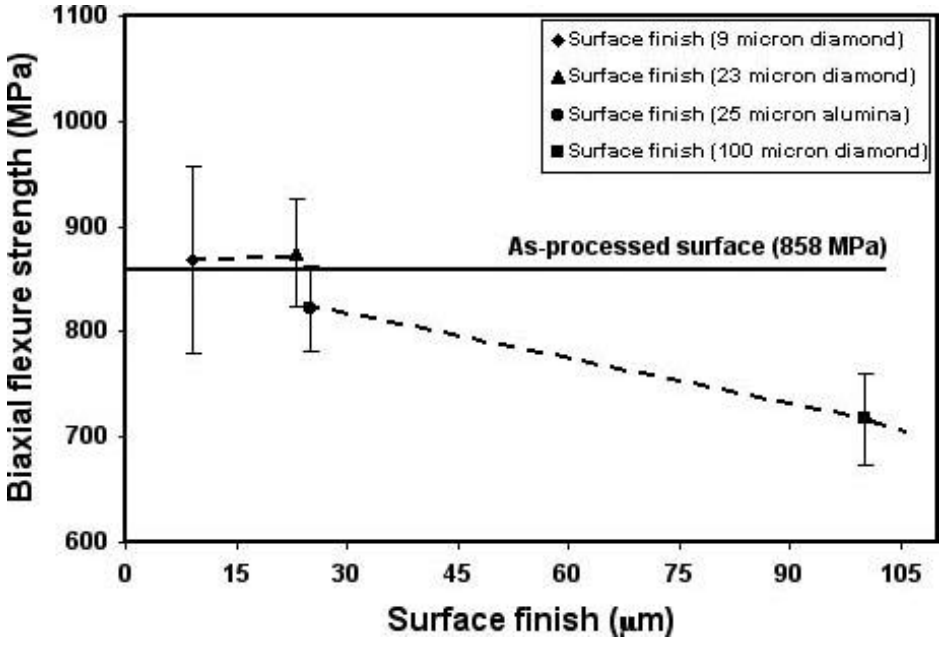

Figure 2. Variation of biaxial flexure strength for specimens with different surface finishes. The ground surfaces were loaded in tension.

surface finish below 23 μm diamond finish. A small variation in strength for the specimen sets in the as-processed condition and those ground with 9 μm and 23 μm diamond media indicates that the critical flaw sizes of these three sets of biaxial specimens are similar. These results clearly indicate that the size of the grinding/machining flaw controls the biaxial strength until the strength value reaches that of the specimens in as-processed condition, beyond which, the as-processed surface flaw acts as the strength-controlling flaw, and strength remains unchanged.

Fig. 3 shows the strength distribution plots for the five sets of specimens tested. The Weibull modulus (m) for the specimens with as-processed surface is 12, while it is 14 and 20 for the specimens ground with 23 μm and 9 μm diamond powder, respectively. A small modulus value of 12 for the specimens with as-processed surface indicates a large variation in critical flaw size. The Weibull moduli of the specimens ground with 100 μm diamond powder and 25 μm alumina powder have not been calculated because, to date, only a few specimens (less than 10) have been tested in these two sets. The Weibull distribution for specimens ground with 100 μm diamond powder indicates that for a given stress (strength) value, the probability of failure is much higher as compared with the other sets (with finer surface finish).

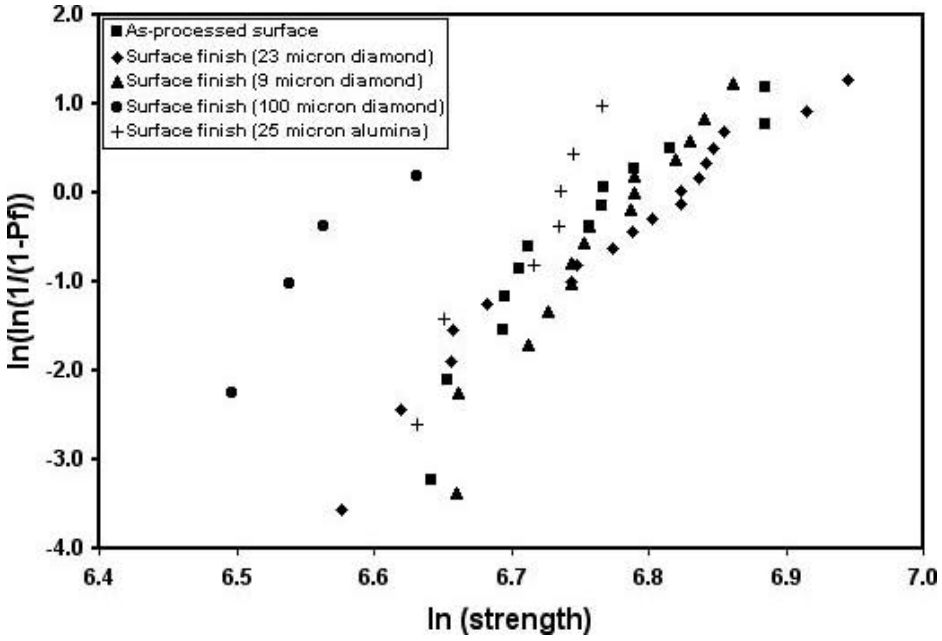

Figure 3. Weibull distribution of biaxial strength for specimens with different surface finishes.

Fractographic evaluation of the fractured biaxial specimens was performed to characterize the strength controlling flaws in the five sets of specimens. Fig. 4 shows a typical fracture surface of an as-processed specimen. The fracture initiation site (the region below the marked boundary in the figure) is a processing induced flaw with pores. Fig. 5 shows typical fracture surfaces of ground specimens showing machining

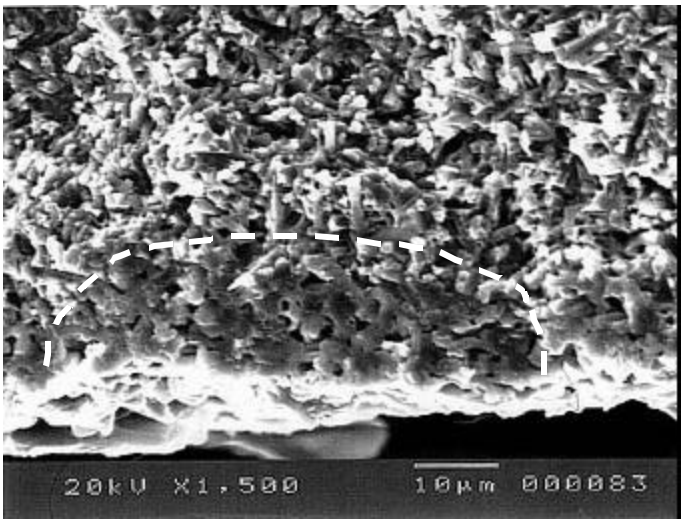

Figure 4. SEM micrograph of the fracture surface of the biaxial test specimen with as-processed surface in tension. The region bounded by the dotted line represents processing induced surface flaw at fracture initiation site.

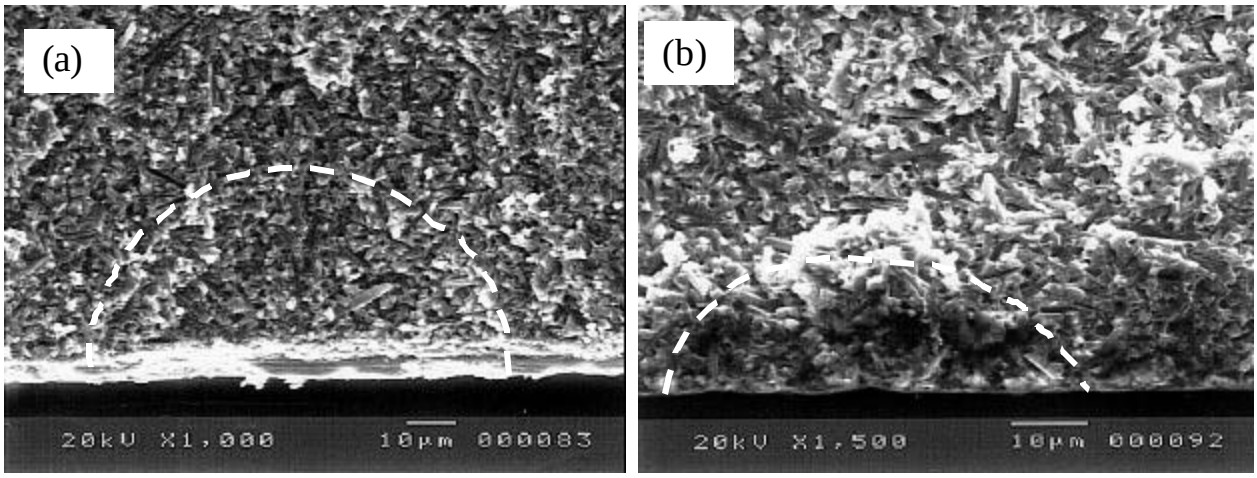

Figure 5. SEM micrographs of the fracture surface of the biaxial specimens (a) ground with 100 µm diamond powder and (b) ground with 23 µm diamond powder. The regions bounded by the dotted lines represent machining flaws at the fracture initiation sites.

flaws (regions bounded by the dotted line) at the fracture initiation sites. These results clearly suggest that processing flaws control the strength in as-processed specimens whereas machining flaws dictate the strength in the ground specimens.

The variation of biaxial flexure strength as a function of critical flaw size is shown in Fig. 6 for the as-processed specimens and the specimens ground with diamond powder. In some specimens, the critical flaw sizes were measured by measuring the depth of the sharp machining flaws while in others the fracture mirror radii were measured and subsequently the critical flaw sizes were calculated using equation (2)[2]:

$$A_o/C_o = 13 \qquad (2)$$

where A_o is the fracture mirror radius and C_o is the critical flaw size. Fig. 6 shows that the critical flaw sizes in the specimens ground with 100 μm diamond powder are much larger than the other three sets of specimens. This is consistent with the lower strength of the specimens ground with 100 μm diamond powder as seen in Fig. 2.

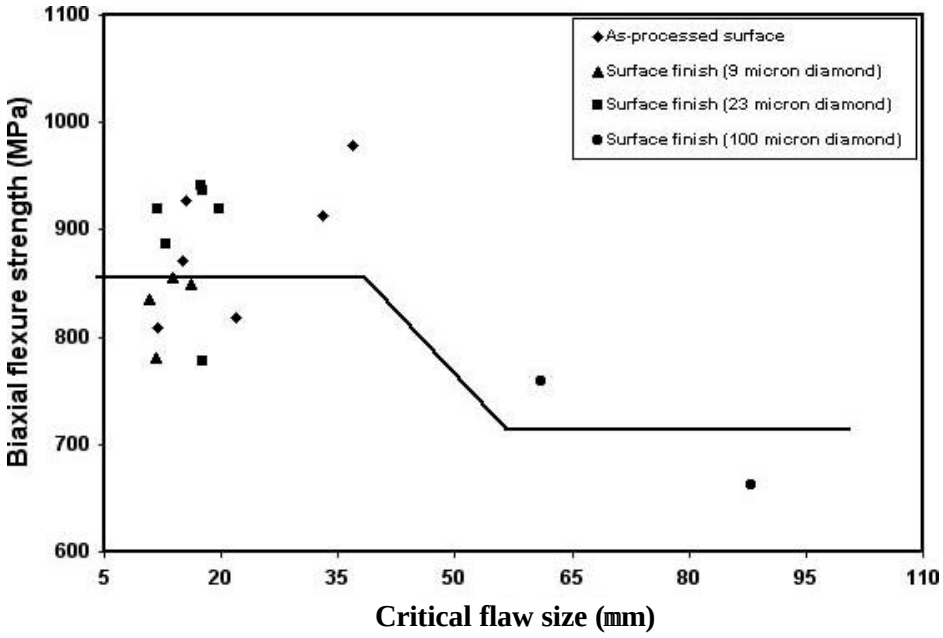

Figure 6. Variation of biaxial flexure strength with measured critical flaw size. The larger flaw sizes of the biaxial specimens (ground with 100 μm diamond powder) results in lower strength.

Table-I compares the biaxial and four-point flexural strength for AS800 Si_3N_4 specimens with as-processed and ground (25 μm alumina powder) surfaces in tension. As evident from the table, the four-point flexural strength is significantly lower as compared to the biaxial flexure strength in both the as-processed and the ground specimens. This is primarily due to the fact that failure of the four-point specimens initiated from corner cracks and large surface defects as was reported in the previous quarterly report. The corner cracks may have been subjected to higher stress concentration as compared with biaxial specimens in which failure initiated from flat surfaces. These results suggest that

the biaxial flexure testing reflects the true strength of the material better than the four-point flexure test.

Table-I Comparison of Four-point and Biaxial Flexure Strength

Specimen	Four-point flexure strength (MPa)	Biaxial flexure strength (MPa)
As-processed surface in tension	459 ± 102	858 ± 68
Ground surface in tension (25 μm alumina powder)	689 ± 67	822 ± 41

(B) Verifying the analytical stress solution by stress measurements using piezofluorescence (M. K. Ferber and M. Lance, Oak Ridge National Laboratory)

This reporting period the AD995 flexure specimens, which were fabricated from several billets of an AD995 aluminum oxide ceramic manufactured by CoorsTek, Golden, CO., were fractured at room temperature. The average strength was 304 ± 29 MPa. Fig. 7 illustrates the Weibull plot.

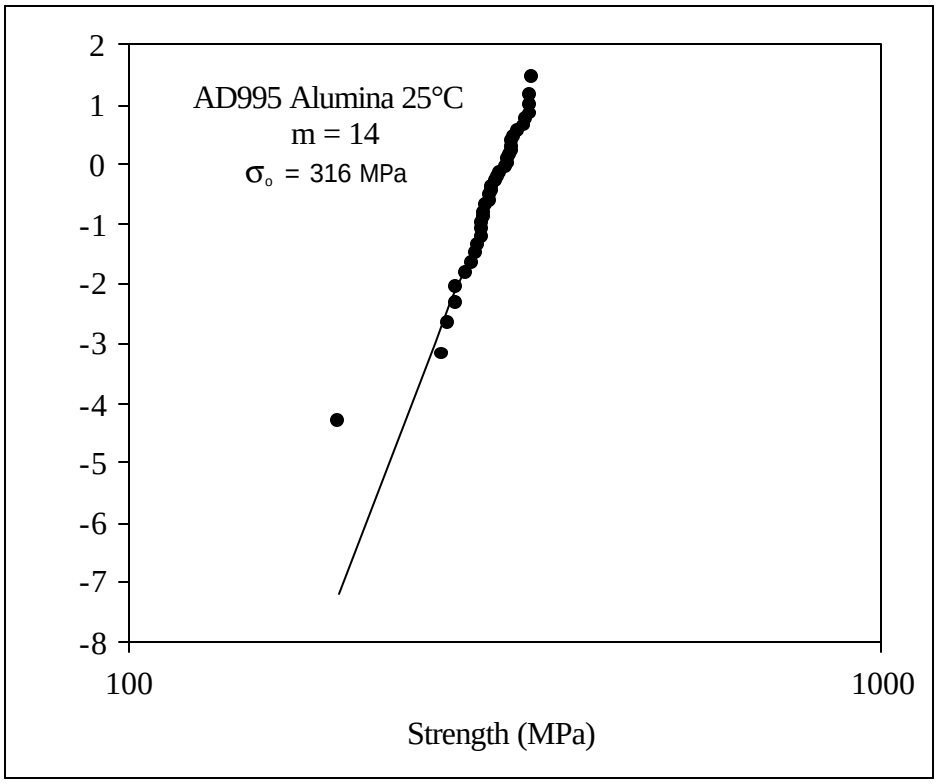

Figure 7. Weibull plot obtained from the room-temperature flexure strength tests of the AD995.

The choice of aluminum oxide was motivated by the fact that stresses can be measured on the microscopic scale using the technique of piezofluorescence. The Dilor XY800 Raman microprobe at Oak Ridge National Laboratory (ORNL) was used to conduct these measurements. This instrument is equipped with a confocal line imaging system, which allows the user to map out areas on the surface of a material while maintaining the confocality of the instrument thereby limiting the depth penetration. The system is entirely automated for imaging material surfaces. Also, the software allows for the processing of large amounts of spectra by a simple curve fitting routine whereby the same curve fitting parameters are automatically applied to all spectra. This greatly reduces analysis time since each spectra doesn't need to be processed individually. Loading fixtures and heating/cooling stages can be used *in situ.*

The experimental setup used to measure stress profiles along the tensile surface of the biaxial disks is shown in Fig. 8. The objective lens is focused on the tensile surface of the specimen. The approximate spatial resolution is 2 μm. To measure stress profiles, the load stage can be moved in the horizontal plane by means of x-y position stages (not shown).

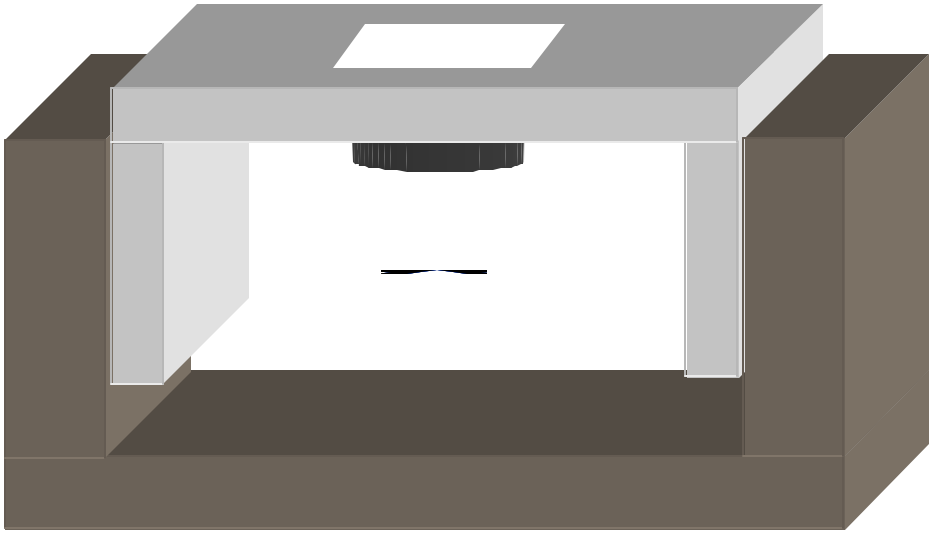

Figure 8. Fixture used to apply constant loads to the biaxial disks. The objective lens is part of the Raman system.

Preliminary measurements are shown in Fig. 9. The predicted biaxial stress profile was calculated using the expressions

$$\sigma_r = 3P\,(1+\nu)/(4*\pi*t^2)(2\ln(a/r)+(1-\nu)/(2\,(1+\nu))*[(a/r)^2-1)\,(b/R)^2 \quad (3a)$$

$$\sigma_\theta = 3P\,(1+\nu)/(4*\pi*t^2)\,(2\ln(a/r)+(1-\nu)/(2\,(1+\nu))*[4-(b/r)^2]\,(a/R)^2 \quad (3b)$$

where σ_r is the radial stress, σ_θ is the tangential stress, r is the radial position, P is the load, a is the radius of the support "ring", b is the effective radius of contact of the loading ball on the specimen, R is the specimen radius, t is the specimen thickness, and ν is Poisson's ratio. The biaxial stress, $(\sigma_r + \sigma_\theta)/2$, was calculated assuming b was approximately equal to t/3.

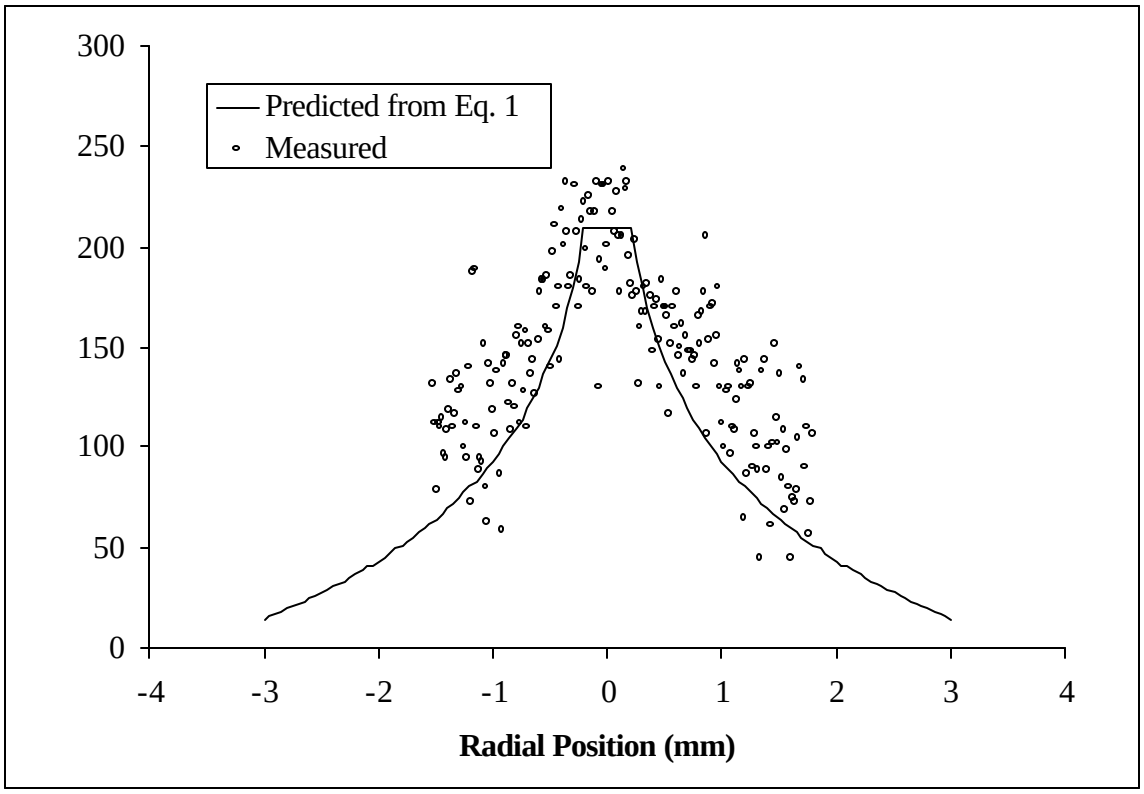

Figure 9. Comparison of predicted and measured profiles of the biaxial stress for a biaxial specimen loaded at 30 N.

As shown in Fig. 9, there was considerable scatter in the experimental stress values determined from the piezofluorescence measurements. Given that the laser spot size (1-2 μm) was small compared with the average grain size of the alumina (10-20 μm), this point-to-point variation was most likely a result of the local residual stress variations associated with the individual grains. These micro-stresses are generated due to the thermal expansion anisotropy of the alumina. In spite of this scatter, the experimental and predicted biaxial stress values were in good agreement. The piezofluorescence measurements are currently being repeated using a fine-grain alumina.

References:

[1] R. Thiruvengadaswamy and R. O. Scattergood, “Biaxial flexure testing of brittle materials” Scripta Metallurgica, vol. 25 (1991), pp. 2529-2532.
[2] J. J. Mecholsky Jun, S. W. Freimam and R. W. Rice, “Fracture surface analysis of ceramics” Journal of Material Science, vol. 11 (1976), pp. 1310-1319.